

Infrared Intensity-Carrying Modes and Electron–Vibration Interactions in the Radical Cations of Polycyclic Aromatic Hydrocarbons

Hajime Torii* and Yuko Ueno

Department of Chemistry, School of Science, The University of Tokyo, Bunkyo-ku, Tokyo 113-0033, Japan

Akira Sakamoto and Mitsuo Tasumi

Department of Chemistry, Faculty of Science, Saitama University, Urawa, Saitama 338-8570, Japan

Received: February 1, 1999; In Final Form: May 7, 1999

Electron–vibration interactions giving rise to infrared (IR) intensities characteristic of the radical cations of polycyclic aromatic hydrocarbons (PAHs) are examined theoretically. Density functional calculations are performed for the radical cations of naphthalene, anthracene, tetracene, pentacene, pyrene, perylene, and phenanthrene at the B3LYP/6-311G* level. A theoretical formulation for analyzing the vibrational motions giving rise to strong IR intensities is presented. It is shown from the algebraic properties of the expression for IR intensities that three vibrational degrees of freedom responsible for all the IR intensities of a given molecule, called the intensity-carrying modes, can be derived from dipole derivatives in the Cartesian coordinate system. By using this theory, the origin of the IR intensities may be examined even when it is difficult to define an appropriate nonredundant set of internal coordinates. For molecules with C_{2v} or higher symmetry (including D_{2h}), each intensity-carrying mode belongs to each of the three IR-active symmetry species. It is shown that the vibrational patterns of the intensity-carrying modes and the directions of their dipole derivatives in the PAH radical cations are explained by the following two mechanisms. One is the mechanism involving *long-range charge flux* between distant benzene rings. By this mechanism, the vibrational motion of each ring occurs in the direction of the structural change between the neutral and charged benzene, and the vibrational motions of distant rings are combined out of phase to give rise to long-range charge flux. The other involves *short-range charge flux* within each benzene ring. The relation between vibrational motion and charge flux induced by this mechanism is explained by regarding the benzene radical cation as building “blocks” constituting the molecule and considering the intensity-carrying modes of each block. In both cases, the phase relationship of the singly occupied molecular orbital (SOMO) determines which of the two Jahn–Teller distorted structures of the benzene radical cation should be considered. It may be said, therefore, that the vibrational patterns of the intensity-carrying modes and the directions of their dipole derivatives are closely related to the electronic structures.

1. Introduction

The infrared (IR) spectra of the radical cations of polycyclic aromatic hydrocarbons (PAHs) have been studied extensively during the past decade.^{1–16} By using the matrix-isolation technique, the IR spectra have been observed for the radical cations of linear polyacenes ranging from naphthalene to pentacene as well as other PAHs such as pyrene, perylene, phenanthrene, chrysene, and coronene.^{2–11} Calculations of the IR spectra of these radical cations have been performed by using the *ab initio* restricted open-shell Hartree–Fock (ROHF)^{3,5,12} and the density functional^{13,14} methods.

It has been shown in these studies that the features of the IR spectra of the PAH radical cations are substantially different from those of the neutral PAHs. In the case of the PAH radical cations, the IR intensities of some bands in the fingerprint region (1700–950 cm^{-1} , corresponding to the CC stretches and the CH in-plane bends) are much larger than those of the bands observed below 950 cm^{-1} (the CH out-of-plane bends), and the bands at $\sim 3000 \text{ cm}^{-1}$ (the CH stretches) are very weak. By contrast, in the IR spectra of the neutral PAHs, the intensities of the bands in the 1700–950- cm^{-1} region are significantly smaller than those of the bands observed below 950 cm^{-1} , and

the bands at $\sim 3000 \text{ cm}^{-1}$ are very strong. The IR intensity patterns observed for the PAH radical cations are interesting from the astronomical viewpoint,^{1,15,16} since the IR radiation from the interstellar medium is strong in the fingerprint region, and PAHs are accordingly expected to be positively charged in the interstellar medium.

The IR intensity patterns characteristic of the PAH radical cations have been well reproduced by ROHF^{3,5,12} and even better by density functional calculations.^{13,14} It has been demonstrated in ref 14 for many PAH radical cations (as well as neutral PAHs) that good agreement between the observed and calculated IR spectra can be obtained by density functional calculations. However, the mechanism giving rise to these spectral features has not been clarified. Ionization-induced enhancement of the IR intensities of the bands in the fingerprint region is not restricted to the case of PAHs. For example, the IR band arising from the bond-alternation mode (or the so-called effective conjugation mode¹⁷) of charged polyenes, in which neighboring CC bonds stretch and contract alternately, is substantially more intense than the corresponding band of the neutral species.^{17–20} Elucidation of the mechanism which induces these strong IR bands is interesting from the viewpoint^{17,21} that strong IR intensities in general (on the order of 10^2 km mol^{-1} or larger) cannot be explained only by static polarization of the relevant

* Corresponding author. E-mail: torii@chem.s.u-tokyo.ac.jp.

bonds, and hence some intimate interplay between the vibrational and electronic motions is necessary for the generation of strong IR intensities. In our previous study,²¹ a theory based on a two-state model Hamiltonian is presented for analyzing the electron–vibration interaction in the molecular skeleton of charged polyenes and related molecules. In this theory, one vibrational degree of freedom (along the bond-alternation coordinate), two diabatic electronic states, and the coupling between the two states are considered, and the charge flux in the molecular skeleton, which is the origin of the strong IR intensities in the fingerprint region and is induced by the electron–vibration interaction, is examined. In the case of the PAH radical cations also, the electron–vibration interaction is expected to be important for the enhancement of the IR intensities. However, application of the above theory²¹ to the case of the PAH radical cations is not straightforward, since the vibrational patterns giving rise to strong IR intensities are not evident from the molecular structures alone, in contrast to the cases of charged polyenes and other molecules with linear conjugated π -electron systems.

In the present paper, the mechanism giving rise to the IR intensities characteristic of the PAH radical cations is studied theoretically. Density functional calculations are performed for several PAH radical cations of small to intermediate size and for some related species. A theoretical formulation is presented so that the vibrational patterns giving rise to strong IR intensities may be derived from the dipole derivatives calculated by the density functional method. Electron–vibration interactions important for the enhancement of IR intensities are examined by comparing these vibrational patterns and the electronic structures.

2. Theory

An important step toward the goal of elucidating the mechanism for the generation of strong IR intensities is to clarify the vibrational motions responsible for the strong IR intensities. When it is feasible to define an appropriate nonredundant set of internal coordinates (called “molecular symmetry coordinates” in our previous studies^{22–25}), such vibrational motions are easily recognized by examining the dipole derivatives with respect to this set of internal coordinates, which are calculated by the transformation of the dipole derivatives with respect to Cartesian coordinates obtained from ab initio molecular orbital (MO) or density functional calculations. However, for molecules with an intricate network of chemical bonds, e.g., PAHs extended in two dimensions with many fused rings, it is difficult to define an appropriate nonredundant set of internal coordinates. Transformation of dipole derivatives from the Cartesian coordinate basis to the internal coordinate basis cannot be carried out if the set of internal coordinates has redundancy. In some cases, normal modes themselves may be helpful to represent the vibrational motions responsible for strong IR intensities. However, normal modes are determined by the mechanical property (i.e., the vibrational force field) of the molecule, and mixing with relatively “dark” vibrational motions in each normal mode may obscure the origin of the strong IR intensities when there are a few (or many) strongly IR-active normal modes. As shown clearly in refs 22 and 23, the potential energy distribution, which is determined solely by the vibrational force field, is not necessarily a good indicator of the origin of the IR intensity of a normal mode. In this respect, an appropriate “eigenstate-free” formulation is desirable to represent the vibrational motions responsible for IR intensities and hence the electron–vibration interaction terms in a molecular Hamiltonian.

In our previous study,²⁶ a doorway-state theory has been formulated for the purpose of analyzing absorption bands of many-oscillator systems. The name of this theory has been derived from the equivalence in the theoretical framework with a theory of nonradiative electronic relaxation employing the concept of the doorway state.^{27,28} The theory has been applied to the analysis of the amide I bands of globular proteins,²⁹ in which each peptide group in a protein is treated as an oscillator having a transition dipole,³⁰ which represents the amide I vibration. It has been shown that three vibrational degrees of freedom carrying all the IR intensities, called *the intensity-carrying modes* hereafter, can be derived from the vectors representing the transition dipoles.²⁶ The intensity-carrying modes are not equal in general to any of the normal modes. It may be said in this sense that this theory is an “eigenstate-free” formulation.

In this section, the doorway-state theory (the theory of intensity-carrying modes) is reformulated so that it may be employed to characterize the strongly IR-active vibrational motions by using the dipole derivatives with respect to Cartesian coordinates obtained from ab initio MO or density functional calculations. We first define the intensity-carrying modes and discuss the relation between the intensity-carrying-mode picture and the normal-mode picture. Then we discuss the method of calculating the intensity-carrying modes from a given set of dipole derivatives in the Cartesian coordinate system.

A. Definition and Properties of Intensity-Carrying Modes. The IR intensity of normal mode α is expressed as

$$I_{\alpha} = \sum_{i=1}^3 \left(\frac{\partial \mu_i}{\partial Q_{\alpha}} \right)^2 = \sum_{i=1}^3 \left(\sum_{k=1}^m \frac{\partial \mu_i}{\partial x_k} \frac{\partial x_k}{\partial Q_{\alpha}} \right)^2 \quad (1)$$

where $\partial \mu_i / \partial Q_{\alpha}$ is the i th component of the dipole derivative with respect to normal coordinate Q_{α} , with $i = 1, 2, 3$ representing respectively the $x, y,$ and z directions, x_k stands for the mass-weighted Cartesian coordinates, i.e., the Cartesian coordinates weighted by the square root of the atomic masses, and m is the total number of degrees of freedom in a given molecule, which is equal to $3N$, with N being the total number of atoms. We denote the number of vibrational degrees of freedom by n , which is equal to $3N - 5$ for linear molecules and $3N - 6$ otherwise. In the present paper we consider the case of $N \geq 3$.

The summation over k in eq 1 is regarded as the scalar product of two m -dimensional vectors \mathbf{d}_i and \mathbf{q}_{α} defined as

$$\mathbf{d}_i = (\partial \mu_i / \partial x_1, \partial \mu_i / \partial x_2, \dots, \partial \mu_i / \partial x_m) \quad (2)$$

$$\mathbf{q}_{\alpha} = (\partial x_1 / \partial Q_{\alpha}, \partial x_2 / \partial Q_{\alpha}, \dots, \partial x_m / \partial Q_{\alpha}) \quad (3)$$

The last two equations are more concisely expressed as

$$(\mathbf{d}_i)_k = \partial \mu_i / \partial x_k \quad (2a)$$

$$(\mathbf{q}_{\alpha})_k = \partial x_k / \partial Q_{\alpha} \quad (3a)$$

We note that $\mathbf{q}_{\alpha} \mathbf{q}_{\beta} = \delta_{\alpha\beta}$ holds for all α and β . By using the above two vectors, eq 1 is rewritten as

$$I_{\alpha} = \sum_{i=1}^3 (\mathbf{d}_i \mathbf{q}_{\alpha})^2 \quad (4)$$

We will consider an orthogonal transformation from $\{q_\alpha\}_{1 \leq \alpha \leq n}$ to another set of m -dimensional vectors $\{s_\beta\}_{1 \leq \beta \leq n}$. Since $\{d_i\}_{1 \leq i \leq 3}$ generates a three-dimensional subspace in the m -dimensional space, we can take $\{s_\beta\}_{1 \leq \beta \leq n}$ such that

$${}^t d_i s_\beta = 0 \quad (i = 1, 2, 3; 4 \leq \beta \leq n) \quad (5)$$

is satisfied.²⁶ We then define a set of vibrational coordinates S_β as

$$(s_\beta)_k = \partial x_k / \partial S_\beta \quad (6)$$

From eqs 5 and 6 we obtain

$$\sum_{\beta=1}^3 \left(\frac{\partial \mu_i}{\partial S_\beta} \right)^2 = \sum_{\beta=1}^3 ({}^t d_i s_\beta)^2 = \sum_{\beta=1}^n ({}^t d_i s_\beta)^2 = \sum_{\beta=1}^n \left(\frac{\partial \mu_i}{\partial S_\beta} \right)^2 \quad (7)$$

for each i . Since $\{S_\beta\}_{1 \leq \beta \leq n}$ is related to $\{Q_\alpha\}_{1 \leq \alpha \leq n}$ by an orthogonal transformation, it is easily seen that

$$\sum_{\beta=1}^n \left(\frac{\partial \mu_i}{\partial S_\beta} \right)^2 = \sum_{\alpha=1}^n \left(\frac{\partial \mu_i}{\partial Q_\alpha} \right)^2 \quad (8)$$

holds for each i .

From the above equations, it is evident that the set of three vibrational modes $\{S_\beta\}_{1 \leq \beta \leq 3}$ carries all the IR intensities. These vibrational modes are the intensity-carrying modes, and represent the origin of the IR intensities and hence the electron–vibration interactions.

For molecules with C_{2v} or higher symmetry (such as D_{2h}), there are three IR-active symmetry species (if the degenerate IR-active symmetry species, if any, is counted as many times as its degeneracy). In this case, if ${}^t d_i q_\alpha \neq 0$ for certain i and α , then ${}^t d_j q_\alpha = 0$ for $j \neq i$. (For molecules with degenerate IR-active symmetry species, normal modes should be classified by using the symmetry species of the C_{2v} or D_{2h} point group). Since $\{s_\beta\}$ is obtained from an orthogonal transformation of $\{q_\alpha\}$, and there are only three s_β (i.e., $1 \leq \beta \leq 3$) for which ${}^t d_i s_\beta$ may not be zero (eq 5), we can define $\{s_\beta\}$ so that it also has the above property; i.e., if ${}^t d_i s_\beta \neq 0$ for certain i and β , then ${}^t d_j s_\beta = 0$ for $j \neq i$. In other words, there is only one intensity-carrying mode for each IR-active symmetry species. We adopt the numbering of $\{s_\beta\}$ such that ${}^t d_i s_\beta = 0$ for $i \neq \beta$. The three intensity-carrying modes S_1, S_2 , and S_3 defined from this set of s_β and eq 6 are called intensity-carrying modes X, Y, and Z, respectively. It is easily seen from eqs 7 and 8 that $({}^t d_i s_i)^2 [= (\partial \mu_i / \partial S_i)^2]$ is equal to the total IR intensity of the normal modes belonging to the relevant symmetry species. This total IR intensity is distributed to each normal mode according to the projection of the normal mode to the intensity-carrying mode; i.e., $(\partial \mu_i / \partial S_i)^2 \times (\partial S_i / \partial Q_\alpha)^2$ is equal to the IR intensity of normal mode α . Since $\{Q_\alpha\}_{1 \leq \alpha \leq n}$ and $\{S_\beta\}_{1 \leq \beta \leq n}$, when they are supplemented by the normalized translational and rotational coordinates (see below), are related to the mass-weighted Cartesian coordinates $\{x_k\}_{1 \leq k \leq m}$ by an orthogonal transformation, we obtain

$$\begin{aligned} \left(\frac{\partial S_i}{\partial Q_\alpha} \right)^2 &= \left(\sum_{k=1}^m \frac{\partial S_i}{\partial x_k} \frac{\partial x_k}{\partial Q_\alpha} \right)^2 \\ &= \left(\sum_{k=1}^m \frac{\partial x_k}{\partial S_i} \frac{\partial x_k}{\partial Q_\alpha} \right)^2 = ({}^t s_i q_\alpha)^2 \end{aligned} \quad (9)$$

Therefore, $({}^t s_i q_\alpha)^2$ is proportional to the relative IR intensity of each normal mode belonging to the relevant symmetry species.

B. Method of Calculating the Intensity-Carrying Modes. We define six m -dimensional vectors t_i and r_i ($i = 1, 2, 3$) representing the translational and rotational motions such that

$$(t_i)_k = \partial x_k / \partial T_i \quad (10)$$

$$(r_i)_k = \partial x_k / \partial R_i \quad (11)$$

where T_i and R_i are the normalized translational and rotational coordinates, respectively. We note that ${}^t t_i t_j = \delta_{ij}$, ${}^t r_i r_j = \delta_{ij}$, and ${}^t t_i r_j = 0$ hold for all i and j ($1 \leq i, j \leq 3$). All the vectors representing the vibrational motions should be orthogonal to these six vectors. We define w_i ($1 \leq i \leq 3$) as

$$w_i = d_i - \sum_{j=1}^3 \{ ({}^t d_i t_j) t_j + ({}^t d_i r_j) r_j \} \quad (12)$$

It is easily seen that the vectors orthogonal to w_i , t_i , and r_i ($1 \leq i \leq 3$) are also orthogonal to d_i . Therefore, the vectors representing the intensity-carrying modes may be expressed as

$$s_i = w_i / |w_i| \quad (1 \leq i \leq 3) \quad (13)$$

For molecules with C_{2v} or higher symmetry, s_i ($1 \leq i \leq 3$) thus defined are orthogonal to each other and induce dipole derivatives which are also mutually orthogonal.

An alternative way to obtain the intensity-carrying modes may be described as follows. We take an arbitrary set of mutually orthogonal normalized vibrational coordinates E_γ ($1 \leq \gamma \leq n$). In this coordinate system we define an $n \times n$ matrix M given as

$$M_{\beta\gamma} = \sum_{i=1}^3 (\partial \mu_i / \partial E_\beta) (\partial \mu_i / \partial E_\gamma) \quad (14)$$

where $\partial \mu_i / \partial E_\gamma$ is calculated as

$$\partial \mu_i / \partial E_\gamma = \sum_{k=1}^m (\partial \mu_i / \partial x_k) (\partial x_k / \partial E_\gamma) \quad (15)$$

This matrix M is in the same form as the one describing radiative damping interactions (in the long-wavelength limit) in a theory of superradiance of molecular aggregates.^{31,32} To obtain the intensity-carrying modes, it is sufficient to find the matrix of orthogonal transformation from $\{E_\gamma\}$ to $\{S_\beta\}$. For this purpose, we suppose the case where $\{E_\gamma\}$ happens to be $\{S_\beta\}$. From eqs 5 and 6, it is evident that only $M_{\beta\gamma}$ with $1 \leq \beta, \gamma \leq 3$ are nonzero in this case. Therefore, the orthogonal transformation from $\{E_\gamma\}$ to $\{S_\beta\}$ is obtained by diagonalization of M . The eigenvectors corresponding to nonzero eigenvalues represent the intensity-carrying modes, and the other eigenvectors represent the “dark” modes. It is easily seen that $\{S_\beta\}$ thus defined satisfies

$$\sum_{i=1}^3 (\partial \mu_i / \partial S_\beta) (\partial \mu_i / \partial S_\gamma) = 0 \quad (\beta \neq \gamma) \quad (16)$$

i.e., the dipole derivatives with respect to S_β are orthogonal to each other in all cases, in contrast to $\{s_\beta\}$ obtained in the

previous paragraph for which this condition holds only for molecules with C_{2v} or higher symmetry.

3. Computational Procedure

Density functional calculations of dipole derivatives are carried out for the radical cations of naphthalene, anthracene, tetracene, pentacene, perylene, pyrene, and phenanthrene. Becke's three-parameter hybrid method³³ using the Lee–Yang–Parr correlation functional³⁴ (B3LYP) is employed in combination with the 6-311G* basis set. It has been shown that the vibrational wavenumbers and IR intensities calculated by using the B3LYP method are in good agreement with the experimental results for many PAH radical cations¹⁴ as well as the naphthalene radical anion.²³ It is therefore expected that the dipole derivatives calculated in this study are sufficiently reliable.

To support the discussion on the electron–vibration interactions in the PAH radical cations, calculations are also performed for the radical cations of benzene and biphenyl and the *cis,cis*-pentadienyl cation in the 1^1A_1 (ground) and 1^1B_2 (excited) electronic states. For the calculation on the 1^1B_2 state of the pentadienyl cation, the configuration interaction singles (CIS) method³⁵ (one of *ab initio* MO methods) is used in combination with the 6-311G* basis set. All the other calculations are carried out at the B3LYP/6-311G* level. C_{2v} symmetry is assumed for the pentadienyl cation and D_{2h} symmetry for the radical cations of benzene and biphenyl. As a result, each of these species (except for one of the Jahn–Teller distorted structures of the benzene radical cation) has one or two imaginary-wavenumber mode(s). However, calculations on structures with lower symmetry are not necessary for the purpose of the present study.

The vibrational motions giving rise to strong IR intensities are examined by using the formulation described in section 2. Since the molecules treated in this study have C_{2v} or D_{2h} symmetry, one intensity-carrying mode is calculated for each of the three IR-active symmetry species. As described in section 2, each intensity-carrying mode is denoted by X, Y, or Z, according to the direction of the transition dipole induced by the intensity-carrying mode.

All the density functional and *ab initio* MO calculations are performed by using the Gaussian 94 program³⁶ on IBM SP2 computers at the Computer Center of the Institute for Molecular Science. The analyses based on the theory of intensity-carrying modes are performed on a Hitachi M5800/320 computer at the Computer Center of the University of Tokyo.

4. Results and Discussion

A. Benzene Radical Cation and Pentadienyl Cation. Since neutral benzene has a degenerate pair of highest occupied molecular orbitals (HOMOs), there are two Jahn–Teller distorted structures for the benzene radical cation (denoted by structures A and B in Figure 1), depending on the HOMO of neutral benzene from which an electron is removed [i.e., the singly occupied molecular orbital (SOMO) of the radical cation shown in Figure 1c]. The distorted molecular structures are depicted in Figure 1d. The changes in the CC bond lengths occurring upon the transition from the neutral to either structure of the radical cation are determined by the bonding/antibonding character of the SOMO. Since one electron is removed from the SOMO upon the transition from the neutral to the radical cation, a CC bond becomes longer if the SOMO is bonding for the bond and becomes shorter if the SOMO is antibonding. The magnitude of the changes in the CC bond lengths is about 0.03 Å in the case of structure A and about 0.06 Å in the case of structure B. There are four CC bonds in structure B with the

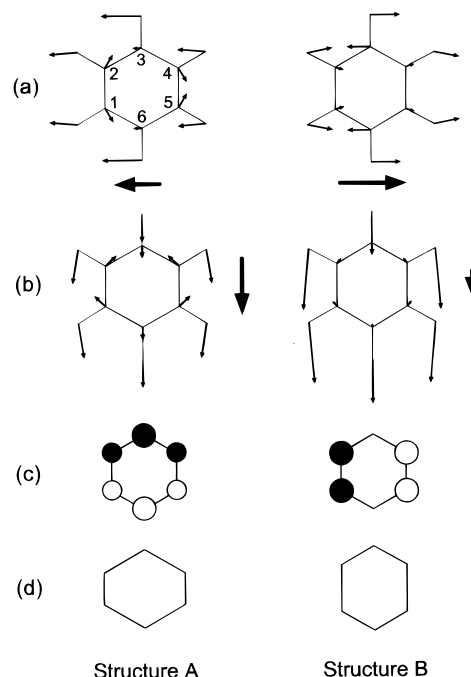


Figure 1. (a) Vibrational pattern of mode Y, (b) vibrational pattern of mode Z, and (c) the singly occupied molecular orbital of the benzene radical cation (left, structure A; right, structure B), with the numbering of the carbon atoms. The thick arrow shown on the side or below the vibrational pattern of each intensity-carrying mode indicates the direction and magnitude of the dipole derivative induced by the vibration. (d) The distorted molecular structures of the benzene radical cation, where the magnitudes of distortion are exaggerated.

nonbonding character of the SOMO. The lengths of these bonds are nearly the same as those in the neutral species.

The calculated vibrational patterns of the in-plane intensity-carrying modes (modes Y and Z) are shown in Figure 1a and 1b, respectively. In the present study, the *x*, *y*, and *z* axes are taken to be the out-of-plane, in-plane horizontal, and in-plane vertical axes, respectively. The out-of-plane intensity-carrying modes (mode X) are not discussed in this study. The carbon atoms are numbered as shown in Figure 1a, for the convenience of comparison with the case of the pentadienyl cation discussed later. The thick arrow shown on the side or below the vibrational pattern of each intensity-carrying mode indicates the direction and magnitude of the dipole derivative induced by the vibration. The arrow is depicted in the direction from the “minus” side to the “plus” side of the dipole derivative, i.e., in the direction of the flux of a positive charge. The magnitudes of the dipole derivatives and the corresponding IR intensities are shown in Table 1 for all the intensity-carrying modes.

The vibrational patterns in Figure 1a,b may seem to indicate that the motions of the hydrogen atoms are more important than those of the carbon atoms in determining the IR intensities. However, it should be noted that the IR intensity of each normal mode is determined by the scalar products between the normal mode and the intensity-carrying modes in the *mass-weighted* Cartesian coordinate system, as shown in eq 9. The vibrational motion of a carbon atom in an intensity-carrying mode is therefore 12 times more important than that of a hydrogen atom if they vibrate by an identical amplitude. In the present case, it is derived from the vibrational patterns shown in Figure 1 that the contribution of the carbon atoms to the dipole derivative is about twice as large as that of the hydrogen atoms for modes Y and Z of structure A and mode Y of structure B. The IR intensity arising from mode Z of structure B is very small because the contribution of the carbon-atom vibrations is small for this

TABLE 1: Dipole Derivatives ($D \text{ \AA}^{-1} \text{ amu}^{-1/2}$) and Infrared Intensities (km mol^{-1}) of the Intensity-Carrying Modes of the Radical Cations of Polycyclic Aromatic Hydrocarbons and Related Species Calculated at the B3LYP/6-311G* Level

species	mode X		mode Y		mode Z	
	dipole deriv	IR int	dipole deriv	IR int	dipole deriv	IR int
benzene radical cation structure A	1.638	113.32	1.614	110.11	1.901	152.76
benzene radical cation structure B	1.635	112.91	2.315	226.48	0.932	36.74
pentadienyl cation ground state	1.690	120.65	3.939	655.53	1.746	128.87
pentadienyl cation excited state	1.846	143.97	2.369	237.14	1.414	84.48
naphthalene radical cation	1.844	143.65	2.669	300.94	1.723	125.50
anthracene radical cation	2.048	177.19	4.221	752.87	1.634	112.87
tetracene radical cation	2.228	209.83	5.732	1388.42	1.604	108.76
pentacene radical cation	2.393	241.98	7.167	2170.72	1.659	116.31
perylene radical cation	2.239	211.75	2.527	269.89	3.517	522.82
biphenyl radical cation	2.079	182.61	1.565	103.46	4.385	812.62
pyrene radical cation	2.094	185.26	3.046	391.99	2.083	183.29
phenanthrene radical cation	2.059	179.20	2.205	205.39	4.371	807.48

intensity-carrying mode. The results shown in Figure 1 therefore demonstrate that the vibrational motions of the carbon atoms play a key role in determining the IR intensities for both structures of the benzene radical cation.

In mode Y of structure A shown in Figure 1a, the C_1-C_2 , C_3-C_4 , and C_5-C_6 bonds stretch while the C_2-C_3 , C_4-C_5 , and C_6-C_1 bonds shrink. Such a vibration of the six-membered ring (if we neglect the motions of the hydrogen atoms) is IR inactive in the case of neutral benzene, because it belongs to the b_{2u} symmetry species of the D_{6h} point group. This mode becomes IR active in the benzene radical cation because of the Jahn–Teller distortion of the molecular structure from D_{6h} to D_{2h} . The vibrational pattern in mode Y of structure B is similar to that in mode Y of structure A in that the C_3-C_4 and C_5-C_6 bonds stretch while the C_2-C_3 and C_6-C_1 bonds shrink. However, the directions of the dipole derivatives induced by these two vibrations are opposite to each other. By contrast, in the case of mode Z, the vibrational patterns calculated for the two structures are similar to each other, and the dipole derivatives induced by these vibrations are in the same direction.

The opposite directions of the dipole derivatives calculated for mode Y of structures A and B suggest that electron–vibration interactions play an important role in generating the dipole derivatives, because the most marked difference between these two structures is in their electronic structures as shown in Figure 1c. Comparison with the results obtained in our previous study²¹ is desirable in this regard. For this purpose, the intensity-carrying modes are calculated also for the 1^1A_1 (ground) and 1^1B_2 (excited) electronic states of the *cis,cis*-pentadienyl cation ($C_5H_7^+$).

The 1^1A_1 state of the pentadienyl cation is derived by removing the electron of the SOMO from the pentadienyl neutral radical. In other words, the 1^1A_1 state of the cation is generated by placing a hole on the SOMO of the neutral radical. Similarly, the 1^1B_2 state of the cation is made by removing one of the electrons from (or placing a hole on) the orbital next to the SOMO of the neutral radical. The orbital of the hole in each state is shown in Figure 2c. For the purpose of the present paper, the electronic structures of the cationic species should be characterized by the orbital of the hole placed upon the transition from the neutral to the cation. Such a way of electronic-structure characterization is considered to be valid, because the very small magnitude of the dipole derivatives induced by the CC stretches in the neutral species may be regarded as originating from mutual cancellation of the contributions of all the π electrons to the dipole derivatives. Hence the total contribution of the π electrons remaining in the ionic species is opposite in sign and has almost the same magnitude as that of the removed electron.

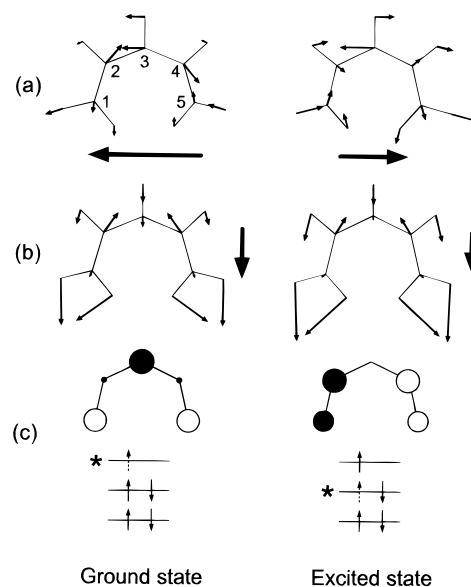


Figure 2. (a) Vibrational pattern of mode Y and (b) vibrational pattern of mode Z of the *cis,cis*-pentadienyl cation (left, the 1^1A_1 state; right, the 1^1B_2 state), with the numbering of the carbon atoms. (c) The molecular orbital from which an electron is removed (i.e., on which a hole is placed) upon the transition from the pentadienyl neutral radical to the pentadienyl cation.

By comparing the phase relationship in the $C_2-C_3-C_4$ part of the orbital of the hole, it is easily recognized that the electronic structure of the 1^1B_2 state of the pentadienyl cation is similar to that of structure B of the benzene radical cation, because the signs of the coefficients on C_2 and C_4 are opposite to each other. The electronic structure of the 1^1A_1 state of the pentadienyl cation is similar to that of structure A of the benzene radical cation. Only the properties of the central part ($C_2-C_3-C_4$) of the pentadienyl cation are examined, because it is expected that there exists an end effect in the properties of the C_1-C_2 and C_4-C_5 parts.²¹

The vibrational patterns of the in-plane intensity-carrying modes calculated for the 1^1A_1 and 1^1B_2 states of the pentadienyl cation are shown in Figure 2a,b. In mode Y (Figure 2a), the C_3-C_4 bond stretches while the C_2-C_3 bond shrinks. The dipole derivative induced by this vibration is directed to the left in the 1^1A_1 state, whereas it is directed to the right in the 1^1B_2 state. Therefore, with regard to the direction of the dipole derivative induced in mode Y, the 1^1A_1 and 1^1B_2 states of the pentadienyl cation are similar to structures A and B, respectively, of the benzene radical cation shown in Figure 1a.

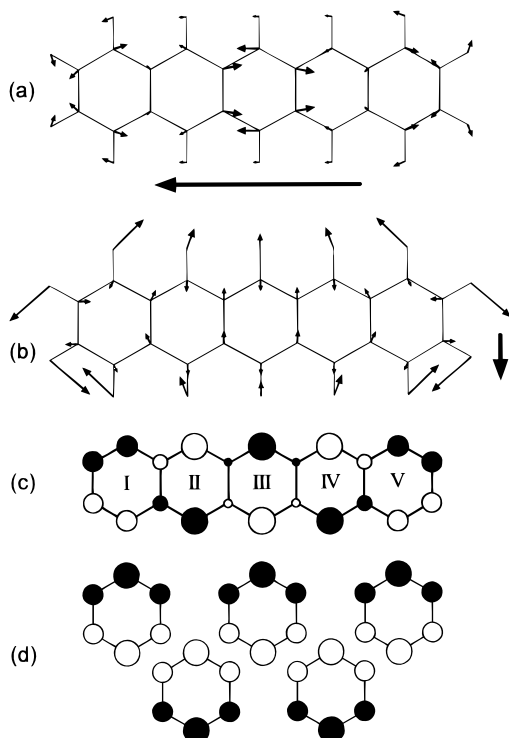


Figure 3. (a) Vibrational pattern of mode Y, (b) vibrational pattern of mode Z, and (c) the singly occupied molecular orbital of the pentacene radical cation, with the numbering of the six-membered rings. (d) Decomposition of the singly occupied molecular orbital of pentacene radical cation into its building blocks.

From the above comparison, it is concluded that the direction of the dipole derivative induced in mode Y is strongly correlated to the electronic structure.

In the case of mode Z (Figure 2b), the vibrational patterns calculated for the two states are similar to each other, and the dipole derivatives induced by these vibrations are in the same direction. This result is consistent with that obtained for the benzene radical cation.

In our previous study,²¹ it has been shown by using a simple model Hamiltonian that the large dipole derivative calculated for the bond-alternation mode (similar to mode Y) of a linear charged polyene arises from a charge flux in the molecular skeleton induced by the strong vibronic coupling between the ground and excited electronic states, and the direction of the dipole derivative in the excited electronic state is opposite to that in the ground electronic state. Since the molecular skeleton of the pentadienyl cation is not cyclically closed, it is possible to apply straightforwardly the results obtained for the model Hamiltonian. From the close relationship between the cases of the benzene radical cation and the pentadienyl cation described above, the opposite directions of the dipole derivatives of mode Y obtained for structures A and B of the benzene radical cation are rationalized. It may be said that the large dipole derivatives calculated for the benzene radical cation originate from intraring charge flux induced by strong vibronic coupling. This type of charge flux is called *short-range charge flux* hereafter.

B. Radical Cations of Linear Polyacenes. The vibrational patterns and the dipole derivatives calculated for the in-plane intensity-carrying modes of the pentacene radical cation are shown in Figure 3a,b. The magnitudes of the dipole derivatives and the corresponding IR intensities are shown in Table 1. The SOMO and the numbering of rings are shown in Figure 3c.

As shown in Table 1, the IR intensity arising from mode Y of the pentacene radical cation is 1 order of magnitude larger

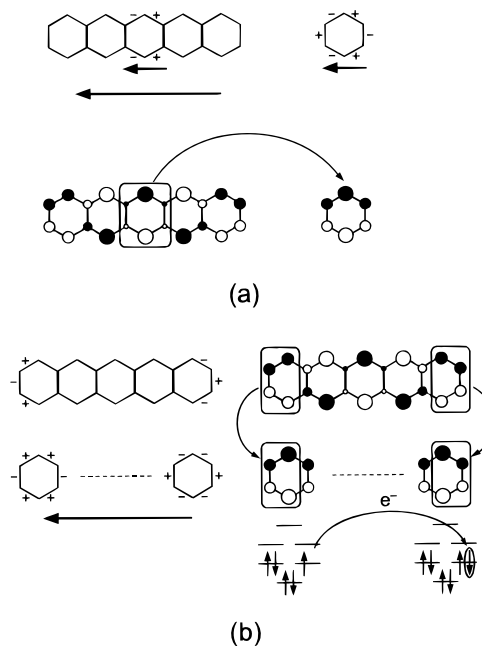


Figure 4. (a) Scheme of the mechanism of short-range charge flux giving rise to the strong IR intensity of mode Y of the pentacene radical cation. The vibrational motion of ring III (the central ring) is explained by the corresponding mode of the benzene radical cation (structure A). (b) Scheme of the mechanism of long-range charge flux. The vibrational motion of the left half of ring I (on the left side of the molecule) is in the direction of the structural change from neutral benzene to structure A of the benzene radical cation, and that of the right half of ring V (on the right side of the molecule) is in the opposite direction. As a result, ring I becomes more cationic and ring V less cationic by this vibration. The charge goes back and forth as the vibration proceeds.

than that arising from mode Z. We therefore concentrate mostly on the mechanisms which generate the large dipole derivative for mode Y. Figure 3a demonstrates that the vibrational motions of the ring in the center (III) as well as those at the ends (I and V) are both important for this mode. By multiplying the dipole derivative tensor ($\partial\mu_i/\partial x_k$) with the vibrational motions in this mode ($\partial x_k/\partial S_\beta$), it may be derived that about 55% of the total dipole derivative induced by mode Y ($\partial\mu_i/\partial S_\beta$) is explained by the vibrational motion of ring III, and about 35% by those of rings I and V. The vibrational motions of the hydrogen atoms explain only about 3% of the total dipole derivative in this case. Therefore, the IR intensities arising from the CH stretches and the in-plane CH bends are very small.

The vibrational motion of ring III in mode Y is explained in the following, where the benzene radical cation is regarded as building blocks constituting the molecule and the appropriate intensity-carrying mode (mode Y in this case) of each block is considered. Concerning the electronic structure, each ring in the pentacene radical cation is similar to that of structure A of the benzene radical cation as shown in Figure 3c,d; the coefficients of the SOMO for the atoms on the boundaries of rings are small because of the cancellation of the contributions from the rings on both sides. We therefore regard structure A of the benzene radical cation as building blocks for the pentacene radical cation. As shown in Figure 4a, it is evident that the relation between the direction of the dipole derivative and the vibrational motion of ring III is the same as that of structure A. This result indicates that short-range charge flux is generated in ring III by the vibrational motion of mode Y. This is one of the important mechanisms by which large dipole derivatives are generated by the CC stretches in the PAH radical cations.

However, the dipole derivatives induced by the vibrational motions of rings I and V in mode Y cannot be explained by this mechanism. As described above, these rings are similar to structure A of the benzene radical cation in their electronic structures. Based on the above mechanism, it may seem as if the vibrational motions of rings I and V in mode Y shown in Figure 3a induce dipole derivatives directed to the right. These vibrational motions nonetheless generate about 35% of the total dipole derivative of mode Y, which is directed to the left. A different mechanism should be introduced to explain this result.

By comparing with Figure 1d, it is noticed that the vibrational motion of (the left half of) ring I in mode Y is in the direction of the structural change from neutral benzene to structure A of the benzene radical cation. Ring I therefore becomes more cationic by this vibration. On the contrary, ring V becomes less cationic by this vibration, because this ring vibrates in the opposite phase. As a result, charge flux is generated between these two rings, as shown in Figure 4b. Of course, the charge goes back and forth as the vibration proceeds. This type of charge flux is called *long-range charge flux* hereafter. This mechanism is considered to be also important for understanding the vibrational motions giving rise to strong IR intensities in the PAH radical cations.

It should be stressed that the above explanation not only shows that the IR intensity of mode Y arises from flux of electric charge, but also demonstrates that the relation among the vibrational pattern of mode Y, the direction of its dipole derivative, and the electronic structure is reasonably well explained by the mechanisms involving long-range charge flux and short-range charge flux.

As explained in section 2A, the relative IR intensity of each normal mode is proportional to its projection to the intensity-carrying mode belonging to the relevant symmetry species, expressed as $(\langle s_i q_\alpha \rangle)^2$ in eq 9. To examine the situation for the b_{2u} modes of the pentacene radical cation, the vibrational patterns of four strongly IR-active normal modes are shown in Figure 5.³⁷

The strongest IR intensity is generated by the 1418.3-cm⁻¹ mode (unscaled wavenumber). The vibrational pattern of this normal mode (Figure 5d) is similar to that of mode Y (Figure 3a), especially in the phase relationship among the vibrations of rings I, III, and V, although the vibration of ring III in the 1418.3-cm⁻¹ mode is smaller in magnitude than that in mode Y. The value of $(\langle s_i q_\alpha \rangle)^2$ is 0.38, indicating that the 1418.3-cm⁻¹ mode carries 38% of the total IR intensity of the b_{2u} modes. The vibrational motion of ring III is significantly large in the 1450.8-cm⁻¹ mode as shown in Figure 5c. This normal mode is similar to mode Y as far as the vibrational motion of ring III is concerned, but the phase relationship between the vibration of ring III and those of rings I and V in the former is opposite to that in the latter. As a result, $(\langle s_i q_\alpha \rangle)^2$ is as small as 0.08. The vibrational motion of ring III in the 1553.7-cm⁻¹ mode (Figure 5b) seems less similar to that of mode Y as compared with that of the 1450.8-cm⁻¹ mode. However, $(\langle s_i q_\alpha \rangle)^2$ is calculated to be as large as 0.20 for the 1553.7-cm⁻¹ mode, because the phase relationship among the vibrations of rings I, III, and V in this normal mode is the same as that in mode Y. The vibrational pattern of the 1583.9-cm⁻¹ mode (Figure 5a) does not seem to be quite similar to that of mode Y. However, mainly because of the vibrations in the left half of ring I and the right half of ring V, the value of $(\langle s_i q_\alpha \rangle)^2$ is calculated to be 0.10 for this normal mode. In total, the four modes shown in Figure 5 carry 76% of the total IR intensity of the b_{2u} modes. The other normal modes generate smaller IR intensities than these four normal modes.

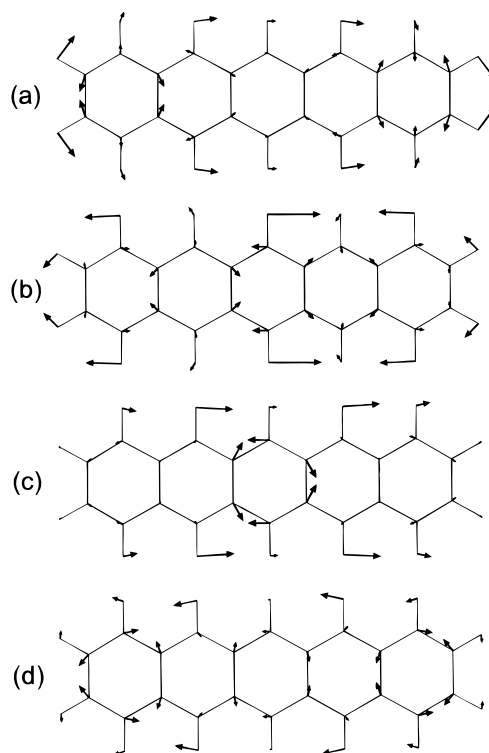


Figure 5. Vibrational patterns of strongly IR-active normal modes of the pentacene radical cation calculated at (a) 1583.9, (b) 1553.7, (c) 1450.8, and (d) 1418.3 cm⁻¹.

From the IR intensities and the vibrational patterns of normal modes, one might conclude that the vibration of ring III is not very important for generating IR intensities, because the IR intensity of the 1450.8-cm⁻¹ mode (Figure 5c) is moderate. However, as shown in Figure 3a, the vibration of ring III is actually more important than those of rings I and V for generating IR intensities. The intensity-carrying-mode picture is thus useful for directly inspecting the vibrational motions responsible for the IR intensities.

The vibrational motions in mode Y of the radical cations of other linear polyacenes (naphthalene, anthracene, and tetracene) may be explained in the same way as those of the pentacene radical cation. We take the case of the naphthalene radical cation as an example. As shown in Figure 6c, the electronic structures of both rings (I and II) are similar to that of structure A of the benzene radical cation. The vibrational motion of ring I in mode Y shown in Figure 6a, in which the C₅-C₆, C₇-C₈, C₈-C₉, and C₅-C₁₀ bonds stretch, is in the direction of the structural change from neutral benzene to structure A of the benzene radical cation. The vibrational motion of ring II is in the opposite phase. The large dipole derivative calculated for mode Y of the naphthalene radical cation is therefore explained by the mechanism involving long-range charge flux described above.

As shown in Table 1, the dipole derivatives of mode Y of the radical cations of linear polyacenes (naphthalene, anthracene, tetracene, and pentacene) are approximately proportional to the number of rings. As a result, the corresponding IR intensities are approximately proportional to the square of the number of rings. This is also an indication that the mechanism of long-range charge flux is important for explaining the IR intensities of these molecules.

The vibrational motions of the carbon atoms in mode Z of the radical cations of linear polyacenes (e.g., Figures 3b and 6b) are explained simply by short-range charge fluxes in the benzene rings, i.e., by applying the vibration of mode

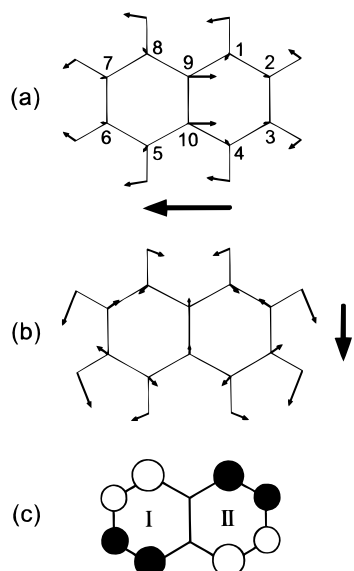


Figure 6. (a) Vibrational pattern of mode Y, (b) vibrational pattern of mode Z, and (c) the singly occupied molecular orbital of the naphthalene radical cation.

Z of structure A of the benzene radical cation to each ring of the radical cations of linear polyacenes. The IR intensity of mode Z is almost constant for this series of molecules as shown in Table 1, indicating that only short-range charge flux is important for this mode.

C. Radical Cations of Perylene and Biphenyl. Perylene is regarded as being made of two biphenyl molecules condensed with two common CC bonds, or made of two naphthalene molecules connected by two CC bonds. In this section, the results obtained for the perylene radical cation are discussed in relation to those obtained for the radical cations of biphenyl and naphthalene.

The vibrational patterns of the in-plane intensity-carrying modes, the corresponding dipole derivatives, and the SOMO calculated for the radical cations of perylene and biphenyl are shown in Figures 7 and 8. The numbering of the carbon atoms constituting ring III and some neighboring atoms in the perylene radical cation is also shown in Figure 7a. The electronic structure of the part consisting of rings I and IV (or rings II and V) of the perylene radical cation is similar to that of the biphenyl radical cation. It is also evident that the electronic structure of the part consisting of rings I and II (or rings IV and V) of the perylene radical cation is similar to that of the naphthalene radical cation (Figure 6c). Except for ring III of the perylene radical cation, all the rings of the radical cations of perylene, biphenyl, and naphthalene correspond to structure A of the benzene radical cation with regard to their electronic structures. In view of the strong correlation between the electronic structures and the vibrational patterns of the intensity-carrying modes obtained in sections 4A and 4B, it is expected that the vibrational patterns of the intensity-carrying modes of the radical cations of perylene, biphenyl, and naphthalene are mutually related.

The mechanism giving rise to the large dipole derivatives for mode Z of the radical cations of perylene and biphenyl is schematically shown in Figure 9. In this intensity-carrying mode (Figures 7b and 8b), the rings on the upper half of the molecule vibrate in the direction of the structural change from neutral benzene to structure A of the benzene radical cation. The rings on the lower half of the molecule vibrate in the opposite phase. As a result, long-range charge fluxes occur in mode Z. The

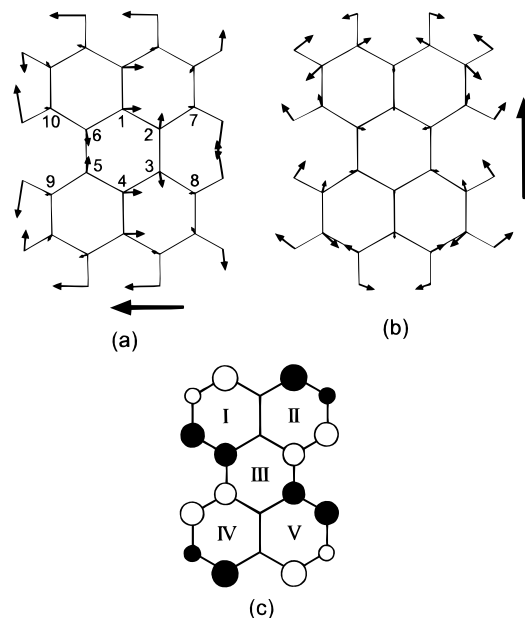


Figure 7. (a) Vibrational pattern of mode Y, (b) vibrational pattern of mode Z, and (c) the singly occupied molecular orbital of the perylene radical cation.

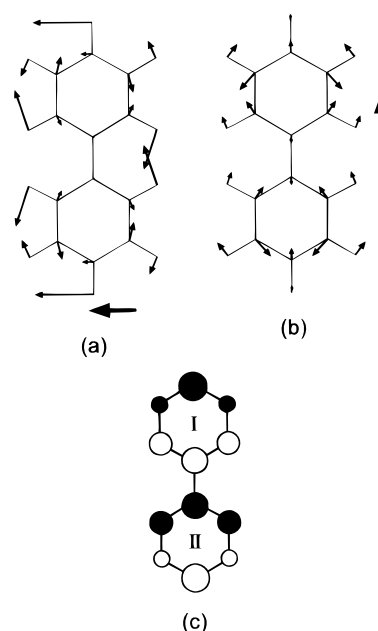


Figure 8. (a) Vibrational pattern of mode Y, (b) vibrational pattern of mode Z, and (c) the singly occupied molecular orbital of the biphenyl radical cation (planar structure).

directions of the dipole derivatives calculated for these radical cations are consistent with the scheme shown in Figure 9.

In the case of mode Y, however, the vibrational patterns calculated for the radical cations of perylene and biphenyl are different from each other (Figures 7a and 8a), especially in the vibrations of the C₂–C₃, C₅–C₆, C₂–C₇, C₃–C₈, C₅–C₉, and C₆–C₁₀ bonds in Figure 7a and the corresponding bonds in Figure 8a. We note that the vibrational motions of the carbon atoms should be mainly considered, because the vibrational motion of a carbon atom in an intensity-carrying mode is 12 times more important than that of a hydrogen atom if they vibrate by an identical amplitude as explained in section 4A. The vibrational patterns of both rings of the biphenyl radical cation are similar to that of structure A of the benzene radical cation (Figure 1a, left), indicating that short-range (intra-ring)

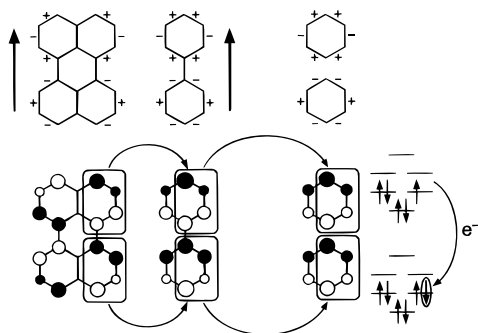


Figure 9. Scheme of the mechanism of long-range charge flux giving rise to the strong IR intensities of mode Z of the radical cations of perylene and biphenyl. The vibrational motions of the rings on the upper half of the molecules are in the direction of the structural change from neutral benzene to structure A of the benzene radical cation, and those of the rings on the lower half of the molecules are in the opposite direction. As a result, the former become more cationic and the latter less cationic by these vibrations. The charge goes back and forth as the vibration proceeds.

charge fluxes are generated. By contrast, the vibrational pattern calculated for the part consisting of rings I and II (or rings IV and V) of the perylene radical cation is rather similar to that of the naphthalene radical cation (Figure 6a). As explained in section 4B, charge fluxes between the rings are generated in this case. The vibrational motions of the C_2-C_3 and C_5-C_6 bonds of the perylene radical cation shown in Figure 7a need additional explanations. These vibrational motions as part of the intensity-carrying mode cannot be inferred from those of the benzene radical cation, because the electronic structure of ring III of the perylene radical cation is not similar to that of either structure of the benzene radical cation. It is most easy to understand these vibrational motions by considering that they induce (long-range) charge flux between two “biphenyl parts”, i.e., rings I and IV connected by the C_5-C_6 bond, and rings II and V connected by the C_2-C_3 bond. As shown in a previous study on the structures and vibrational modes of biphenyl and its ionic species,³⁸ the inter-ring C–C bond of the biphenyl radical cation is shorter than that of neutral biphenyl. Therefore, by the vibrational motions of the C_2-C_3 and C_5-C_6 bonds shown in Figure 7a, the “biphenyl part” on the left becomes more cationic than the one on the right. This scheme is consistent with the direction of the dipole derivative calculated for this intensity-carrying mode. It is related to the mechanism giving rise to intermolecular charge flux in the dimer of the TTF radical cation and other related species, which is the origin of the IR bands characteristic of dimeric species.^{39–41}

D. Radical Cations of Pyrene and Phenanthrene. The vibrational patterns of the in-plane intensity-carrying modes, the corresponding dipole derivatives, and the SOMO calculated for the pyrene radical cation are shown in Figure 10. In contrast to the cases of the radical cations of linear polyacenes, perylene, and biphenyl, the electronic structures of all the rings constituting the pyrene radical cation are similar to that of structure B of the benzene radical cation. As a result, the relation between the vibrational motions and the dipole derivatives in the intensity-carrying modes of the pyrene radical cation is expected to be different from that discussed in sections 4B and 4C.

The mechanism giving rise to the large dipole derivative for mode Z is schematically shown in Figure 11. In this intensity-carrying mode (Figure 10b), ring I vibrates in the direction of the structural change from neutral benzene to structure B of the benzene radical cation. Ring III vibrates in the opposite phase. As a result, a long-range charge flux occurs in this

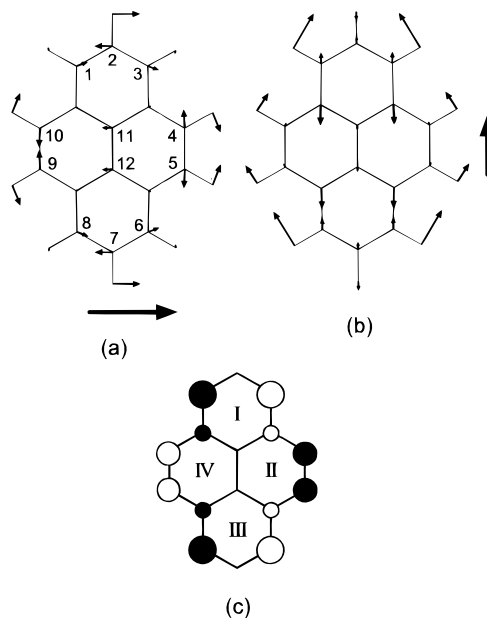


Figure 10. (a) Vibrational pattern of mode Y, (b) vibrational pattern of mode Z, and (c) the singly occupied molecular orbital of the pyrene radical cation.

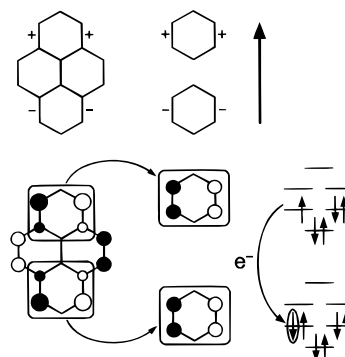


Figure 11. Scheme of the mechanism of long-range charge flux giving rise to the strong IR intensity of mode Z of the pyrene radical cation. The vibrational motion of ring I (the ring on the top) is in the direction of the structural change from neutral benzene to structure B of the benzene radical cation, and that of ring III (the ring on the bottom) is in the opposite direction. As a result, the former becomes more cationic and the latter less cationic by this vibration. The charge goes back and forth as the vibration proceeds.

intensity-carrying mode. The part consisting of rings I and III (connected by the $C_{11}-C_{12}$ bond) of pyrene may look similar to biphenyl from the structural point of view. However, the vibrational motions in the intensity-carrying modes of the radical cations of these molecules are quite different from each other since the electronic structures are different.

For mode Y of the pyrene radical cation, the relation between the vibrational motions (Figure 10a) and the direction of the dipole derivative is explained in the following way. The vibrational motions of rings I and III, especially the $C_1-C_2-C_3$ and $C_6-C_7-C_8$ parts, are rationalized by comparing them with those calculated for structure B of the benzene radical cation (Figure 1a, right). Short-range charge fluxes occur in these rings. By contrast, as a result of the vibrational motions of the C_4-C_5 and C_9-C_{10} bonds, ring II is displaced in the direction of the structural change from neutral benzene to structure B of the benzene radical cation, and ring IV in the opposite direction. The $C_{11}-C_{12}$ bond does not stretch or contract in this intensity-carrying mode because rings II and IV have this bond in common. Therefore, a charge flux is generated between rings

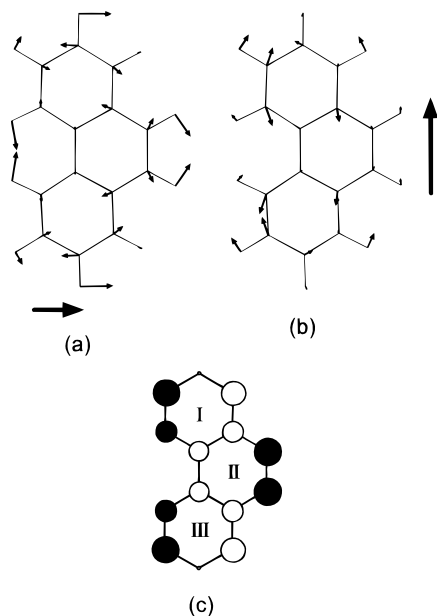


Figure 12. (a) Vibrational pattern of mode Y, (b) vibrational pattern of mode Z, and (c) the singly occupied molecular orbital of the phenanthrene radical cation.

II and IV by the mechanism of long-range charge flux. The direction of the dipole derivative calculated for this intensity-carrying mode is consistent with this scheme.

The vibrational patterns of the in-plane intensity-carrying modes, the corresponding dipole derivatives, and the SOMO calculated for the phenanthrene radical cation are shown in Figure 12. It is evident that the electronic structure of this radical cation is similar to that of the pyrene radical cation. As a result, the vibrational patterns in both of the in-plane intensity-carrying modes of the former are similar to those of the latter.

5. Concluding Remarks

In the present study, the origin of the strong IR intensities characteristic of the PAH radical cations is examined theoretically. The vibrational patterns giving rise to the strong IR intensities are analyzed. It is shown that the mechanism of long-range charge flux as well as that of short-range charge flux, both related to electron–vibration interactions, are important for the strong IR intensities. For discussing the relation between the vibrational motions of the intensity-carrying modes and the directions of the dipole derivatives, it is necessary to consider the electronic structures of the radical cations, especially the phase relationship of the SOMO. It may be said that detailed examination of both the electronic and vibrational properties is essential for understanding the IR intensities (and probably the Raman intensities as well) of charged species.

References and Notes

- (1) Allamandola, L. J.; Tielens, A. G. G. M.; Barker, J. R. *Astrophys. J.* **1985**, *290*, L25.
- (2) Szczepanski, J.; Roser, D.; Personette, W.; Eyring, M.; Pellow, R.; Vala, M. *J. Phys. Chem.* **1992**, *96*, 7876.
- (3) Szczepanski, J.; Vala, M.; Talbi, D.; Parisel, O.; Ellinger, Y. *J. Chem. Phys.* **1993**, *98*, 4494.
- (4) Szczepanski, J.; Chapo, C.; Vala, M. *Chem. Phys. Lett.* **1993**, *205*, 434.
- (5) Vala, M.; Szczepanski, J.; Pauzat, F.; Parisel, O.; Talbi, D.; Ellinger, Y. *J. Phys. Chem.* **1994**, *98*, 9187.
- (6) Szczepanski, J.; Wehlburg, C.; Vala, M. *Chem. Phys. Lett.* **1995**, *232*, 221.
- (7) Szczepanski, J.; Drawdy, J.; Wehlburg, C.; Vala, M. *Chem. Phys. Lett.* **1995**, *245*, 539.
- (8) Hudgins, D. M.; Sandford, S. A.; Allamandola, L. J. *J. Phys. Chem.* **1994**, *98*, 4243.
- (9) Hudgins, D. M.; Allamandola, L. J. *J. Phys. Chem.* **1995**, *99*, 3033.
- (10) Hudgins, D. M.; Allamandola, L. J. *J. Phys. Chem.* **1995**, *99*, 8978.
- (11) Hudgins, D. M.; Allamandola, L. J. *J. Phys. Chem. A* **1997**, *101*, 3472.
- (12) Pauzat, F.; Talbi, D.; Miller, M. D.; DeFrees, D. J.; Ellinger, Y. *J. Phys. Chem.* **1992**, *96*, 7882.
- (13) Ho, Y.-P.; Yang, Y.-C.; Klippenstein, S. J.; Dunbar, R. C. *J. Phys. Chem.* **1995**, *99*, 12115.
- (14) Langhoff, S. R. *J. Phys. Chem.* **1996**, *100*, 2819.
- (15) Szczepanski, J.; Vala, M. *Nature* **1993**, *363*, 699.
- (16) Cook, D. J.; Schlemmer, S.; Balucani, N.; Wagner, D. R.; Steiner, B.; Saykally, R. J. *Nature* **1996**, *380*, 227.
- (17) Gussoni, M.; Castiglioni, C.; Zerbi, G. *Spectroscopy of Advanced Materials; Advances in Spectroscopy 19*; Clark, R. J. H., Hester, R. E., Eds.; Wiley: New York, 1991; p 251.
- (18) Fincher, Jr., C. R.; Ozaki, M.; Heeger, A. J.; MacDiarmid, A. G. *Phys. Rev. B* **1979**, *19*, 4140.
- (19) Harada, I.; Furukawa, Y.; Tasumi, M.; Shirakawa, H.; Ikeda, S. *J. Chem. Phys.* **1980**, *73*, 4746.
- (20) Piaggio, P.; Dellepiane, D.; Piseri, L.; Tubino, R.; Taliani, C. *Solid State Commun.* **1984**, *50*, 947.
- (21) Torii, H.; Tasumi, M. *J. Phys. Chem. B* **1997**, *101*, 466.
- (22) Furuya, K.; Inagaki, Y.; Torii, H.; Furukawa, Y.; Tasumi, M. *J. Phys. Chem. A* **1998**, *102*, 8413.
- (23) Torii, H.; Sakamoto, A.; Ueno, Y.; Tasumi, M., manuscript in preparation.
- (24) Torii, H.; Tasumi, M. *J. Mol. Struct. (THEOCHEM)* **1995**, *334*, 15.
- (25) Torii, H.; Tasumi, M.; Bell, I. M.; Clark, R. J. H. *Chem. Phys.* **1997**, *216*, 67.
- (26) Torii, H.; Tasumi, M. *J. Chem. Phys.* **1992**, *97*, 86.
- (27) Mukamel, S.; Jortner, J. *Excited States*; Lim, E. C., Ed.; Academic: New York, 1977; Vol. 3, p 57.
- (28) Mukamel, S. *J. Phys. Chem.* **1985**, *89*, 1077.
- (29) Torii, H.; Tasumi, M. *J. Chem. Phys.* **1992**, *97*, 92.
- (30) Torii, H.; Tasumi, M. *J. Chem. Phys.* **1992**, *96*, 3379.
- (31) Lehmborg, R. H. *Phys. Rev. A* **1970**, *2*, 883.
- (32) Spano, F. C.; Mukamel, S. *J. Chem. Phys.* **1989**, *91*, 683.
- (33) Becke, A. D. *J. Chem. Phys.* **1993**, *98*, 5648.
- (34) Lee, C.; Yang, W.; Parr, R. G. *Phys. Rev. B* **1988**, *37*, 785.
- (35) Foresman, J. B.; Head-Gordon, M.; Pople, J. A.; Frisch, M. J. *J. Phys. Chem.* **1992**, *96*, 135.
- (36) Frisch, M. J.; Trucks, G. W.; Schlegel, H. B.; Gill, P. M. W.; Johnson, B. G.; Robb, M. A.; Cheeseman, J. R.; Keith, T.; Petersson, G. A.; Montgomery, J. A.; Raghavachari, K.; Al-Laham, M. A.; Zakrzewski, V. G.; Ortiz, J. V.; Foresman, J. B.; Cioslowski, J.; Stefanov, B. B.; Nanayakkara, A.; Challacombe, M.; Peng, C. Y.; Ayala, P. Y.; Chen, W.; Wong, M. W.; Andres, J. L.; Replogle, E. S.; Gomperts, R.; Martin, R. L.; Fox, D. J.; Binkley, J. S.; Defrees, D. J.; Baker, J.; Stewart, J. J. P.; Head-Gordon, M.; Gonzalez, C.; Pople, J. A. *Gaussian 94*; Gaussian, Inc.: Pittsburgh, PA, 1995.
- (37) The normal modes of the pentacene radical cation are calculated at the B3LYP/4-31G level because of the limitation in the available computational resources. The intensity-carrying modes calculated at this level are essentially the same as those calculated at the B3LYP/6-311G* level.
- (38) Furuya, K.; Torii, H.; Furukawa, Y.; Tasumi, M. *J. Mol. Struct. (THEOCHEM)* **1998**, *424*, 225.
- (39) Tanner, D. B.; Jacobsen, C. S.; Bright, A. A.; Heeger, A. J. *Phys. Rev. B* **1977**, *16*, 3283.
- (40) Bozio, R.; Zanon, I.; Girlando, A.; Pecile, C. *J. Chem. Phys.* **1979**, *71*, 2282.
- (41) Meneghetti, M.; Pecile, C. *J. Chem. Phys.* **1996**, *105*, 397.